

Decoupled Visual Servoing from a set of points imaged by an omnidirectional camera

Hicham Hadj-Abdelkader*, Youcef Mezouar* and Philippe Martinet**[‡]

Abstract—This paper presents a hybrid decoupled vision-based control scheme valid for the entire class of central catadioptric sensors (including conventional perspective cameras). First, we consider the structure from motion problem using imaged 3D points. Geometrical relationships are exploited to enable a partial Euclidean reconstruction by decoupling the interaction between translation and rotation components of a homography matrix. The information extracted from the homography are then used to design a control law which allow us to fully decouple rotational motions from translational motions. Real time experimental results using an eye-to-hand robotic system with a paracatadioptric camera are presented and confirm the validity of our approach.

I. INTRODUCTION

Vision-based servoing schemes are flexible and effective methods to control robot motion from camera observations. They are generally classified into three groups, namely position-based, image-based and hybrid-based control [10], [16], [20]. These three schemes make assumptions on the link between the initial, current and desired images since they require correspondences between the visual features extracted from the initial image with those obtained from the desired one. These features are then tracked during the camera (and/or the object) motion. If these steps fail the visually based robotic task can not be achieved [7]. Typical cases of failure arise when matching joint image features is impossible (for example when no joint feature belongs to initial and desired images) or when some parts of the image features get out of the field of view during the servoing. Some methods were investigated to resolve this deficiency based on path planning [21], switching control [8], zoom adjustment [24], geometrical and topological considerations [9], [26]. However, such strategies are sometimes delicate to adapt to a generic setup. Conventional cameras suffer thus from restricted field of view. There is thus significant motivation for increasing the field of view of the cameras [4]. Many applications in vision-based robotics, such as mobile robot localization [5] and navigation [29], can benefit from the panoramic field of view provided by omnidirectional cameras. In the literature, there have been several methods proposed for increasing the field of view of cameras systems [4]. One effective way is to combine mirrors with conventional imaging system. The obtained sensors are referred

to as catadioptric imaging systems. The resulting imaging systems have been termed central catadioptric when a single projection center describes the world to image mapping. From a theoretical and practical view point, a single center of projection is a desirable property for an imaging system [1]. Baker and Nayar in [1] derive the entire class of catadioptric systems with a single viewpoint. Clearly, visual servoing applications can also benefit from such sensors since the latter naturally overcome the visibility constraint. Vision-based control of robotic arms, single mobile robot or formation of mobile robots appear thus in the literature with omnidirectional cameras (refer for example to [3], [6], [23], [28],[22]). Image-based visual servoing with central catadioptric cameras using points was studied in [3]. The use of straight lines has also been investigated in [22]. As it is well known, the catadioptric projection of a 3D line in the image plane is a conic curve. In [22], the authors propose to use directly the coordinates of the polar lines of the image center with respect to the conic curves to define the input of the vision-based control scheme. This paper is concerned with homography-based visual servo control techniques with central catadioptric cameras. This framework, also called 2 1/2 D visual servoing [20] in the case where the image features are points, exploits a combination of reconstructed Euclidean information and image features in the control design. The 3D information is extracted from an homography matrix relating two views of a reference plane. As a consequence, the 2 1/2 D visual servoing scheme does not require any 3D model of the target. Unfortunately, in such approach when conventional cameras are used, the image of the target is not guaranteed to remain in the camera field of view. To overcome this deficiency 2 1/2 D visual servoing has been extended to an entire class of omnidirectional cameras in [15]. The resulting interaction matrices are triangular with partial decoupling properties (refer to [20], [15]).

In this paper a new approach for homography-based visual servoing using points imaged with any type of central camera is presented. The structure from motion problem using imaged 3D points is first studied. Geometrical relationships are exploited to linearly estimate a generic homography matrix from which a partial Euclidean reconstruction is obtained. The information extracted from the homography are then used to design a control law which allow us to fully decouple rotational motions from translational motions (*i.e* the resulting interaction matrix is square block-diagonal). Real time experimental results using an eye-to-hand robotic system are presented and confirm the validity of our approach.

* is with LASMEA - UMR 6602 du CNRS
24, avenue des Landais, 63177 Aubiere Cedex - France
hadj,mezouar,martinet@univ-bpclermont.fr
[‡] is with ISRC - Intelligent Systems Research Center
Sungkyunkwan University, Suwan, South Korea
martinet@skku.edu

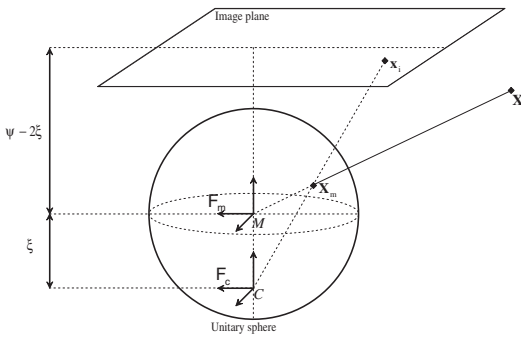


Fig. 1. Central catadioptric image formation

II. MODELISATION

The central catadioptric projection can be modeled by a central projection onto a virtual unitary sphere, followed by a perspective projection onto an image plane. This virtual unitary sphere is centered in the principal effective view point and the image plane is attached to the perspective camera. In this model, called unified model and proposed by Geyer and Daniilidis in [13], conventional perspective camera appears as a particular case.

A. Projection of point

Let \mathcal{F}_c and \mathcal{F}_m be the frames attached to the conventional camera and to the mirror respectively, respectively. In the sequel, we suppose that \mathcal{F}_c and \mathcal{F}_m are related by a simple translation along the Z -axis (\mathcal{F}_c and \mathcal{F}_m have the same orientation as depicted in Figure 1). The origins C and M of \mathcal{F}_c and \mathcal{F}_m will be termed optical center and principal projection center respectively. The optical center C has coordinates $[0 \ 0 \ -\xi]^T$ with respect to \mathcal{F}_m and the image plane $Z = f \cdot (\psi - 2\xi)$ is orthogonal to the Z -axis where f is the focal length of the conventional camera and ξ and ψ describe the type of sensor and the shape of the mirror, and are function of mirror shape parameters (refer to [2]).

Consider the virtual unitary sphere centered in M as shown in Fig.1 and let \mathcal{X} be a 3D point with coordinates $\mathbf{X} = [X \ Y \ Z]^T$ with respect to \mathcal{F}_m . The world point \mathcal{X} is projected in the image plane into the point of homogeneous coordinates $\mathbf{x}_i = [x_i \ y_i \ 1]^T$. The image formation process can be split in three steps as:

- **First step:** The 3D world point \mathcal{X} is first projected on the unit sphere surface into a point of coordinates in \mathcal{F}_m : $\mathbf{X}_m = \frac{1}{\rho} [X \ Y \ Z]^T$, where

$$\rho = \|\mathbf{X}\| = \sqrt{X^2 + Y^2 + Z^2} \quad (1)$$

The projective ray \mathbf{X}_m passes through the principal projection center M and the world point \mathcal{X} .

- **Second step:** The point \mathbf{X}_m lying on the unitary sphere is then perspective projected on the normalized image plane $Z = 1 - \xi$. This projection is a point of homogeneous coordinates $\underline{\mathbf{x}} = [\mathbf{x}^T \ 1]^T = \mathbf{f}(\mathbf{X})$ (where

$\mathbf{x} = [x \ y]^T$):

$$\underline{\mathbf{x}} = \mathbf{f}(\mathbf{X}) = \left[\frac{X}{Z + \xi\rho} \quad \frac{Y}{Z + \xi\rho} \quad 1 \right]^T \quad (2)$$

- **Third step:** Finally the point of homogeneous coordinates $\underline{\mathbf{x}}_i$ in the image plane is obtained after a plane-to-plane collineation \mathbf{K} of the 2D projective point \mathbf{x} : $\underline{\mathbf{x}}_i = \mathbf{K}\underline{\mathbf{x}}$. The matrix \mathbf{K} can be written as $\mathbf{K} = \mathbf{K}_c\mathbf{M}$ where the upper triangular matrix \mathbf{K}_c contains the conventional camera intrinsic parameters, and the diagonal matrix \mathbf{M} contains the mirror intrinsic parameters:

$$\mathbf{M} = \begin{bmatrix} \psi - \xi & 0 & 0 \\ 0 & \psi - \xi & 0 \\ 0 & 0 & 1 \end{bmatrix}, \quad \mathbf{K}_c = \begin{bmatrix} f_u & \alpha_{uv} & u_0 \\ 0 & f_v & v_0 \\ 0 & 0 & 1 \end{bmatrix}$$

Note that, setting $\xi = 0$, the general projection model becomes the well known perspective projection model.

In the sequel, we assume that $Z \neq 0$. Let us denote $\eta = s\rho/|Z| = s\sqrt{1 + X^2/Z^2 + Y^2/Z^2}$, where s is the sign of Z . The coordinates of the image point can be rewritten as:

$$x = \frac{X/Z}{1 + \xi\eta}; \quad y = \frac{Y/Z}{1 + \xi\eta}$$

By combining the two previous equations, it is easy to show that η is the solution of the following second order equation:

$$\eta^2 - (x + y)^2(1 + \xi\eta)^2 - 1 = 0$$

with the following potential solutions:

$$\eta_{1,2} = \frac{\pm\gamma - \xi(x^2 + y^2)}{\xi^2(x^2 + y^2) - 1} \quad (3)$$

where $\gamma = \sqrt{1 + (1 - \xi^2)(x^2 + y^2)}$. Note that, the sign of η is equal to the sign of Z and then it can be shown (refer to Appendix) that the exact solution is:

$$\eta = \frac{-\gamma - \xi(x^2 + y^2)}{\xi^2(x^2 + y^2) - 1} \quad (4)$$

Equation (4) shows that η can be computed as a function of image coordinates \mathbf{x} and sensor parameter ξ . Noticing that:

$$\mathbf{X}_m = (\eta^{-1} + \xi)\bar{\mathbf{x}} \quad (5)$$

where $\bar{\mathbf{x}} = [\mathbf{x}^T \ \frac{1}{1+\xi\eta}]^T$, we deduce that \mathbf{X}_m can also be computed as a function of image coordinates \mathbf{x} and sensor parameter ξ .

III. SCALED EUCLIDEAN RECONSTRUCTION USING HOMOGRAPHY MATRIX OF CATADIOPTRIC VISION

Several methods were proposed to obtain Euclidean reconstruction from two views [11]. They are generally based on the estimation of the fundamental matrix [18] in pixel space or on the estimation of the essential matrix [17] in normalized space. However, for control purposes, the methods based on the essential matrix are not well suited since degenerate configurations can occur (such as pure rotational motion). Homography matrix and Essential matrix based approaches do not share the same degenerate configurations, for example

pure rotational motion is not a degenerate configuration when using homography-based method. The epipolar geometry of central catadioptric system has been more recently investigated [14], [27]. The central catadioptric fundamental and essential matrices share similar degenerate configurations that those observed with conventional perspective cameras, it is why we will focus on homographic relationship. In the sequel, the collineation matrix \mathbf{K} and the mirror parameter ξ are supposed known. To estimate these parameters the algorithm proposed in [2] can be used. In the next section, we show how we can compute homographic relationships between two central catadioptric views of points.

Let \mathbf{R} and \mathbf{t} be the rotation matrix and the translation vector between two positions \mathcal{F}_m and \mathcal{F}_m^* of the central catadioptric camera (see Figures 2). Consider a 3D reference plane (π) given in \mathcal{F}_m^* by the vector $\pi^{*\top} = [\mathbf{n}^* \ -d^*]$, where \mathbf{n}^* is its unitary normal in \mathcal{F}_m^* and d^* is the distance from (π) to the origin of \mathcal{F}_m^* .

A. Homography matrix from points

Let \mathcal{X} be a 3D point with coordinates $\mathbf{X} = [X \ Y \ Z]^\top$ with respect to \mathcal{F}_m and with coordinates $\mathbf{X}^* = [X^* \ Y^* \ Z^*]^\top$ with respect to \mathcal{F}_m^* . Its projection in the unit sphere for the two camera positions are:

$$\mathbf{X}_m = (\eta^{-1} + \xi)\bar{\mathbf{x}} = \frac{1}{\rho} [X \ Y \ Z]^\top$$

$$\mathbf{X}_m^* = (\eta^{*-1} + \xi)\bar{\mathbf{x}}^* = \frac{1}{\rho} [X^* \ Y^* \ Z^*]^\top$$

Using the homogenous coordinates $\underline{\mathbf{X}} = [X \ Y \ Z \ H]^\top$ and $\underline{\mathbf{X}}^* = [X^* \ Y^* \ Z^* \ H^*]^\top$, we can write:

$$\rho(\eta^{-1} + \xi)\bar{\mathbf{x}} = [\mathbf{I}_3 \ 0] \underline{\mathbf{X}} = [\mathbf{R} \ \mathbf{t}] \underline{\mathbf{X}}^* \quad (6)$$

The distance $d(\mathcal{X}, \pi)$ from the world point \mathcal{X} to the plane (π) is given by the scalar product $\pi^{*\top} \cdot \underline{\mathbf{X}}^*$ and:

$$d(\mathbf{X}^*, \pi^*) = \rho^*(\eta^{*-1} + \xi)\mathbf{n}^{*\top}\bar{\mathbf{x}}^* - d^*H^*$$

As a consequence, the unknown homogenous component H^* is given by:

$$H^* = \frac{\rho^*(\eta^{*-1} + \xi)}{d^*}\mathbf{n}^{*\top}\bar{\mathbf{x}}^* - \frac{d(\mathbf{X}^*, \pi^*)}{d^*} \quad (7)$$

The homogenous coordinates of \mathcal{X} with respect to \mathcal{F}_m^* can be rewritten as:

$$\underline{\mathbf{X}}^* = \rho^*(\eta^{*-1} + \xi) [\mathbf{I}_3 \ 0]^\top \bar{\mathbf{x}}^* + [\mathbf{0}_{1 \times 3} \ H^*]^\top \quad (8)$$

By combining the Equations (7) and (8), we obtain:

$$\underline{\mathbf{X}}^* = \rho^*(\eta^{*-1} + \xi)\mathbf{A}_\pi^* \bar{\mathbf{x}}^* + \mathbf{b}_\pi^* \quad (9)$$

where

$$\mathbf{A}_\pi^* = \left[\mathbf{I}_3 \ \frac{\mathbf{n}^*}{d^*} \right]^\top \quad \text{and} \quad \mathbf{b}_\pi^* = \left[\mathbf{0}_{1 \times 3} \ -\frac{d(\mathcal{X}, \pi)}{d^*} \right]$$

According to (9), the expression (6) can be rewritten as:

$$\rho(\eta^{-1} + \xi)\bar{\mathbf{x}} = \rho^*(\eta^{*-1} + \xi)\mathbf{H}\bar{\mathbf{x}}^* + \alpha\mathbf{t} \quad (10)$$

with $\mathbf{H} = \mathbf{R} + \frac{\mathbf{t}}{d^*}\mathbf{n}^{*T}$ and $\alpha = -\frac{d(\mathcal{X}, \pi)}{d^*}$.

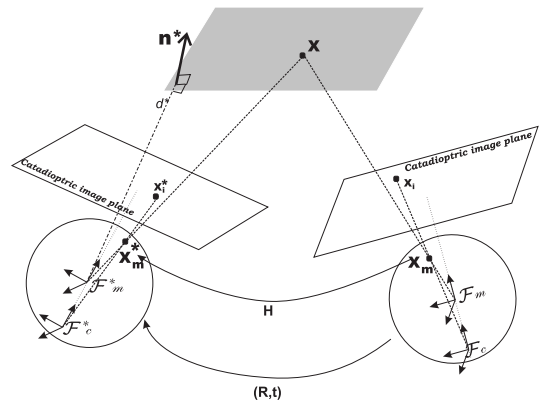


Fig. 2. Geometry of two views of points

\mathbf{H} is the Euclidean homography matrix written as a function of the camera displacement and of the plane coordinates with respect to \mathcal{F}_m^* . It has the same form as in the conventional perspective case (it is decomposed into a rotation matrix and a rank 1 matrix). If the world point \mathcal{X} belongs to the reference plane (π) (i.e. $\alpha = 0$) then Equation (10) becomes:

$$\bar{\mathbf{x}} \propto \mathbf{H}\bar{\mathbf{x}}^* \quad (11)$$

Note that the Equation (11) can be turned into a linear homogeneous equation $\bar{\mathbf{x}} \otimes \mathbf{H}\bar{\mathbf{x}}^* = \mathbf{0}$ (where \otimes denotes the cross-product). As usual, the homography matrix related to (π) , can thus be estimated up to a scale factor, using four couples of coordinates $(\mathbf{x}_k; \mathbf{x}_k^*)$, $k = 1 \dots 4$, corresponding to the projection in the image space of world points \mathcal{X}_k belonging to (π) . If only three points belonging to (π) are available then at least five supplementary points are necessary to estimate the homography matrix by using for example the linear algorithm proposed in [19]. From the estimated homography matrix, the camera motion parameters (that is the rotation \mathbf{R} and the scaled translation $\mathbf{t}_{d^*} = \frac{\mathbf{t}}{d^*}$) and the structure of the observed scene (for example the vector \mathbf{n}^*) can thus be determined (refer to [11], [30]). It can also be shown that the ratio $\sigma = \frac{\rho}{\rho^*}$ can be estimated as follow:

$$\sigma = \frac{\rho}{\rho^*} = (1 + \mathbf{n}^{*T}\mathbf{R}^T\mathbf{t}_{d^*}) \frac{(\eta^{*-1} + \xi)\mathbf{n}^{*T}\bar{\mathbf{x}}^*}{(\eta^{-1} + \xi)\mathbf{n}^{*T}\mathbf{R}^T\bar{\mathbf{x}}} \quad (12)$$

This parameter is used in our 2 1/2 D visual servoing control scheme.

IV. CONTROL SCHEME

As usual when designing a 2 1/2 D visual servoing, the feature vector used as input of the control law combines 2-D and 3-D informations [20]:

$$\mathbf{s} = [\mathbf{s}_i^\top \ \theta \mathbf{u}^\top]^\top$$

where \mathbf{s}_i is a 3-dimensional vector containing the 2D features and, \mathbf{u} and θ are respectively the axis and the rotation angle obtained from \mathbf{R} (rotation matrix between the mirror frame when the camera is in these current and desired positions).

Noticing that the parameter ρ does not depend of the camera orientation and in order to decouple rotational motions from the translational ones, \mathbf{s}_i can be chosen as follow :

$$\mathbf{s}_i = [\log(\rho_1) \log(\rho_2) \log(\rho_3)]^\top$$

where $\rho_{k=1,2,3}$ are the distances from the 3D points $\mathbf{X}_{k=1,2,3}$ to the camera center (refer to equation 1)

The task function \mathbf{e} to regulate to 0 [25] is given by:

$$\mathbf{e} = \mathbf{s} - \mathbf{s}^* = [\Gamma_1, \Gamma_2, \Gamma_3, \theta \mathbf{u}^T]^\top \quad (13)$$

where \mathbf{s}^* is the desired value of \mathbf{s} and $\Gamma_k = \log\left(\frac{\rho_k}{\rho_k^*}\right) = \log(\sigma_k)$, $\{k = 1, 2, 3\}$. The three first components of \mathbf{e} can be estimated using Equation (12). The rotational part of \mathbf{e} is estimated using partial Euclidean reconstruction from the homography matrix derived in Section III. The exponential decay of \mathbf{e} toward $\mathbf{0}$ can be obtained by imposing $\dot{\mathbf{e}} = -\lambda \mathbf{e}$ (λ being a proportional gain), the corresponding control law is:

$$\tau = -\lambda \mathbf{L}^{-1}(\mathbf{s} - \mathbf{s}^*) \quad (14)$$

where τ is a 6-dimensional vector denoting the velocity screw of the central catadioptric camera. It contains the instantaneous angular velocity ω and the instantaneous linear velocity v . \mathbf{L} is the interaction matrix related to \mathbf{s} . It links the variation of \mathbf{s} to the camera velocity: $\dot{\mathbf{s}} = \mathbf{L}\tau$. It is thus necessary to compute the interaction matrix in order to derive the control law given by the Equation (14). The time derivative of the rotation vector $\mathbf{u}\theta$ can be expressed as a function of the catadioptric camera velocity vector τ as:

$$\frac{d(\mathbf{u}\theta)}{dt} = [\mathbf{0}_3 \quad \mathbf{L}_\omega] \tau \quad (15)$$

where \mathbf{L}_ω is given by [20]:

$$\mathbf{L}_\omega(\mathbf{u}, \theta) = \mathbf{I}_3 - \frac{\theta}{2} [\mathbf{u}]_\times + \left(1 - \frac{\text{sinc}(\theta)}{\text{sinc}^2(\frac{\theta}{2})}\right) [\mathbf{u}]_\times^2 \quad (16)$$

with $\text{sinc}(\theta) = \frac{\sin(\theta)}{\theta}$ and $[\mathbf{u}]_\times$ being the antisymmetric matrix associated to vector \mathbf{u} .

To control the 3 translational degrees of freedom, the visual observations and the ratio σ expressed in (12) are used. Consider a 3-D point \mathcal{X}_i , the time derivative of its coordinates, with respect to the current catadioptric frame \mathcal{F}_m , is given by:

$$\dot{\mathbf{X}}_k = [-\mathbf{I}_3 \quad [\mathbf{X}_k]_\times] \tau \quad (17)$$

$[\mathbf{X}_k]_\times$ being the antisymmetric matrix associated to the vector \mathbf{X}_k . The time derivative of Γ_k can be written as:

$$\dot{\Gamma}_k = \frac{\partial \Gamma_k}{\partial \mathbf{X}_k} \dot{\mathbf{X}}_k \quad (18)$$

with:

$$\frac{\partial \Gamma_k}{\partial \mathbf{X}_k} = \frac{1}{\rho^2} [X_k \ Y_k \ Z_k]$$

By combining the equations (17), (18) and (12), it can be shown that:

$$\dot{\mathbf{s}}_i = [\mathbf{A} \quad \mathbf{0}_3] \tau \quad (19)$$

with

$$\mathbf{A} = \begin{pmatrix} \frac{\Phi_1}{\sigma_1 \rho_1^*} & 0 & 0 \\ 0 & \frac{\Phi_2}{\sigma_2 \rho_2^*} & 0 \\ 0 & 0 & \frac{\Phi_3}{\sigma_3 \rho_3^*} \end{pmatrix} \begin{pmatrix} -x_1 & -y_1 & \frac{\xi^2(x_1^2+y_1^2)-1}{1+\gamma_1\xi} \\ -x_2 & -y_2 & \frac{\xi^2(x_2^2+y_2^2)-1}{1+\gamma_2\xi} \\ -x_3 & -y_3 & \frac{\xi^2(x_3^2+y_3^2)-1}{1+\gamma_3\xi} \end{pmatrix} \quad (20)$$

where $\Phi_k = \frac{1+\gamma_k\xi}{\gamma_k+\xi(x_k^2+y_k^2)}$. The task function \mathbf{e} (see Equation (13)) can thus be regulated to $\mathbf{0}$ using the control law (14) with the following interaction matrix \mathbf{L} :

$$\mathbf{L} = \begin{bmatrix} \mathbf{A} & \mathbf{0}_3 \\ \mathbf{0}_3 & \mathbf{L}_\omega \end{bmatrix} \quad (21)$$

In practice, an approximated interaction matrix $\hat{\mathbf{L}}$ is used. The parameter ρ^* can be estimated only once during a off-line learning stage.

V. EXPERIMENTAL RESULTS



Fig. 3. Experimental setup : eye-to-hand configuration

The proposed control law has been tested on a six d-o-f eye-to-hand system (refer to Figure 3). In this configuration, the interaction matrix has to take into account the mapping from the camera frame onto the robot control frame [12]. If we denote $[\mathbf{R}_e, \mathbf{t}_e]$ this mapping, the eye-to-hand interaction matrix \mathbf{L}_e is related to the eye-in-hand one \mathbf{L} by :

$$\mathbf{L}_e = \mathbf{L} \begin{bmatrix} \mathbf{R}_e & [\mathbf{t}_e]_\times \mathbf{R}_e \\ \mathbf{0}_3 & \mathbf{R}_e \end{bmatrix} \quad (22)$$

where $[\mathbf{t}_e]_\times$ is the skew symmetric matrix associated with translation vector \mathbf{t}_e . The interaction matrix \mathbf{L}_e is used in the control law (14). The omnidirectional camera used is a parabolic mirror combined with an orthographic lens. Since we were not interested in image processing in this paper, the target is composed of white marks (see Figure 3). The extracted visual features are the image coordinates of the center of gravity of each mark. From an initial position the robot has to reach a desired position known as a desired 2 1/2 D observation vector \mathbf{s}^* . Three experiments are presented :

- First experiment (Figures 4 and 5): rotational motion only ($\theta_{u_x} = 18\text{dg}$, $\theta_{u_y} = 20\text{dg}$, $\theta_{u_z} = 25\text{dg}$),

- second experiment (Figures 6 and 7): translational motion only ($t_x = 0.3$ m, $t_y = -0.4$ m, $t_z = 0.1$ m),
- third experiment (Figures 8 and 9): generic motion ($t_x = 0.5$ m, $t_y = -0.35$ m, $t_z = 0.1$ m, $\theta u_x = 2$ dg, $\theta u_y = 35$ dg, $\theta u_z = 31$ dg).

For each experiment, the images corresponding to the initial and desired configuration, the trajectories of four image points, the error $s_i - s_i^*$, the rotational error $\mathbf{u}\theta$, the translational and the rotational velocities are presented. The convergence of the error $s - s^*$ demonstrates the correct realization of the task. The computed control laws are given in Figures 5(c)-(d),7(c)-(d),9(c)-(d). We can note its satisfactory variations due to the full decoupling between rotational and translational motions.

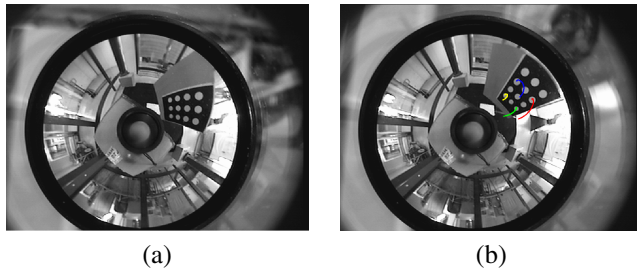


Fig. 4. First experiment: (a) Initial, (b) desired images of the target and trajectories of four image points

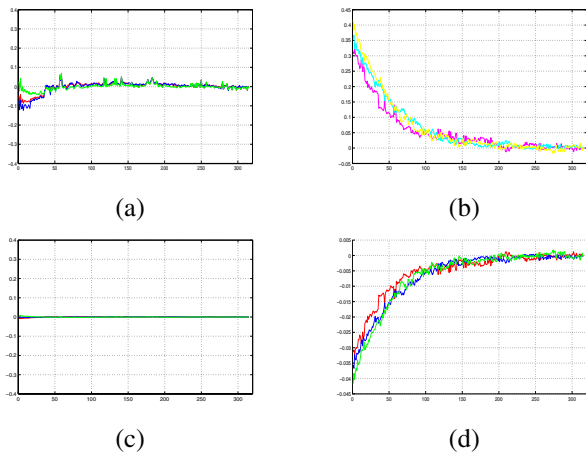


Fig. 5. First experiment: (a) error $s_i - s_i^*$, (b) rotational error $\mathbf{u}\theta$ (rad), (c) translational velocities (m/s) (d) rotational velocities (rad/s)

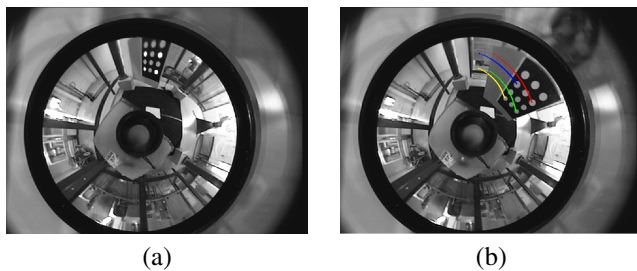


Fig. 6. Second experiment: (a) Initial, (b) desired images of the target and trajectories of four image points

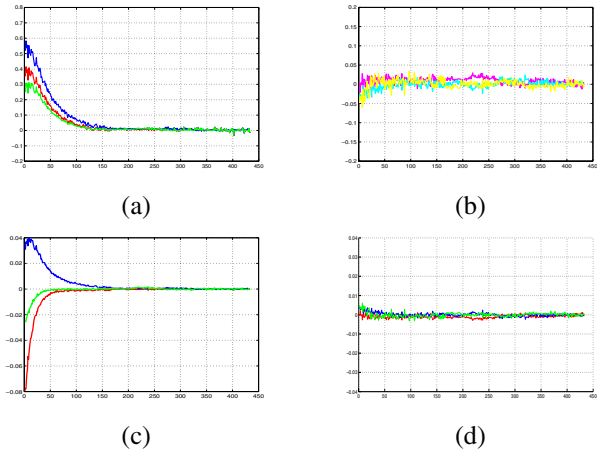


Fig. 7. Second experiment: (a) error $s_i - s_i^*$, (b) rotational error $\mathbf{u}\theta$ (rad), (c) translational velocities (m/s) (d) rotational velocities (rad/s)

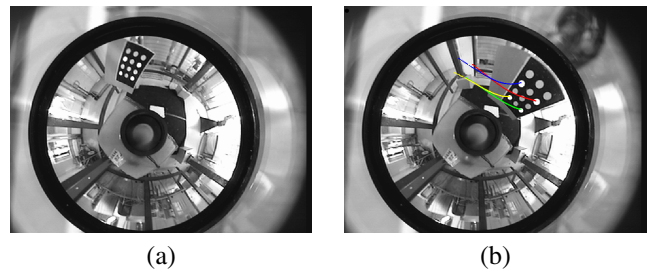


Fig. 8. Third experiment: (a) Initial, (b) desired images of the target and trajectories of four image points

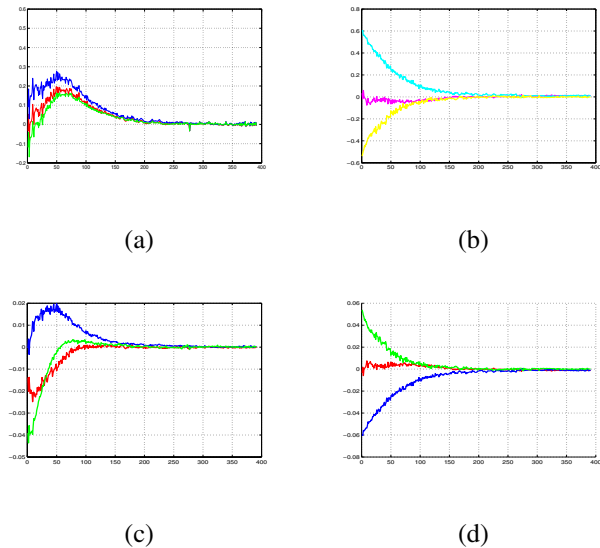


Fig. 9. Third experiment: (a) error $s_i - s_i^*$, (b) rotational error $\mathbf{u}\theta$ (rad), (c) translational velocities (m/s) (d) rotational velocities (rad/s)

VI. CONCLUSION

In this paper a hybrid decoupled vision-based control scheme valid for the entire class of central cameras was presented. Geometrical relationship between two views of imaged points was exploited to estimate a generic homography matrix from which partial Euclidean reconstruction can be obtained. The information extracted from the homography

matrix were then used to design a hybrid control law which allowed us to fully decouple rotational motion from translational motions. Experimental results show the validity of the proposed approach.

REFERENCES

- [1] S. Baker and S. K. Nayar. A theory of single-viewpoint catadioptric image formation. *International Journal of Computer Vision*, 35(2):1–22, November 1999.
- [2] J. Barreto and H. Araujo. Geometric properties of central catadioptric line images. In *7th European Conference on Computer Vision, ECCV'02*, pages 237–251, Copenhagen, Denmark, May 2002.
- [3] J. P. Barreto, F. Martin, and R. Horaud. Visual servoing/tracking using central catadioptric images. In *ISER2002 - 8th International Symposium on Experimental Robotics*, pages 863–869, Bombay, India, July 2002.
- [4] R. Benosman and S. Kang. *Panoramic Vision*. Springer Verlag ISBN 0-387-95111-3, 2000.
- [5] P. Blaer and P.K. Allen. Topological mobile robot localization using fast vision techniques. In *IEEE International Conference on Robotics and Automation*, pages 1031–1036, Washington, USA, May 2002.
- [6] D. Burshka, J. Geiman, and G. Hager. Optimal landmark configuration for vision based control of mobile robot. In *IEEE International Conference on Robotics and Automation*, pages 3917–3922, Taipei, Taiwan, September 2003.
- [7] F. Chaumette. Potential problems of stability and convergence in image-based and position-based visual servoing. *The Confluence of Vision and Control*, D. Kriegman, G. Hager, A. Morse (eds), LNCIS Series, Springer Verlag, 237:66–78, 1998.
- [8] G. Chesi, K. Hashimoto, D. Prattichizzo, and A. Vicino. A switching control law for keeping features in the field of view in eye-in-hand visual servoing. In *IEEE International Conference on Robotics and Automation*, pages 3929–3934, Taipei, Taiwan, September 2003.
- [9] Noah J. Cowan, Joel D. Weingarten, and Daniel E. Koditschek. Visual servoing via navigation functions. *IEEE Transactions on Robotics and Automation*, 18(4):521–533, August 2002.
- [10] B. Espiau, F. Chaumette, and P. Rives. A new approach to visual servoing in robotics. *IEEE Transactions on Robotics and Automation*, 8(3):313–326, June 1992.
- [11] O. Faugeras and F. Lustman. Motion and structure from motion in a piecewise planar environment. *Int. Journal of Pattern Recognition and Artificial Intelligence*, 2(3):485–508, 1988.
- [12] G. Flandin, F. Chaumette, and E. Marchand. Eye-in-hand / eye-to-hand cooperation for visual servoing. In *IEEE Int. Conf. on Robotics and Automation*, San Francisco, CA, Avril 2000.
- [13] C. Geyer and K. Daniilidis. A unifying theory for central panoramic systems and practical implications. In *European Conference on Computer Vision*, volume 29, pages 159–179, Dublin, Ireland, May 2000.
- [14] C. Geyer and K. Daniilidis. Mirrors in motion: Epipolar geometry and motion estimation. In *International Conference on Computer Vision, ICCV03*, pages 766–773, Nice, France, 2003.
- [15] H. Hadj Abdelkader, Y. Mezouar, N. Andreff, and P. Martinet. 2 1/2 d visual servoing with central catadioptric cameras. In *IEEE/RSJ Int. Conf. on Intelligent Robots and Systems, IROS'05*, pages 2342–2347, Edmonton, Canada, August 2005.
- [16] S. Hutchinson, G.D. Hager, and P.I. Corke. A tutorial on visual servo control. *IEEE Transactions on Robotics and Automation*, 12(5):651–670, October 1996.
- [17] H.C. Longuet-Higgins. A computer algorithm for reconstructing a scene from two projections. *Nature*, 293:133–135, September 1981.
- [18] Quang-Tuan Luong and Olivier Faugeras. The fundamental matrix: theory, algorithms, and stability analysis. *Int. Journal of Computer Vision*, 17(1):43–76, 1996.
- [19] E. Malis and F. Chaumette. 2 1/2 d visual servoing with respect to unknown objects through a new estimation scheme of camera displacement. *International Journal of Computer Vision*, 37(1):79–97, June 2000.
- [20] E. Malis, F. Chaumette, and S. Boudet. 2 1/2 d visual servoing. *IEEE Transactions on Robotics and Automation*, 15(2):238–250, April 1999.
- [21] Y. Mezouar and F. Chaumette. Path planning for robust image-based control. *IEEE Transactions on Robotics and Automation*, 18(4):534–549, August 2002.
- [22] Y. Mezouar, H. Haj Abdelkader, P. Martinet, and F. Chaumette. Central catadioptric visual servoing from 3d straight lines. In *IEEE/RSJ Int. Conf. on Intelligent Robots and Systems, IROS'04*, volume 1, pages 343–349, Sendai, Japan, September 2004.
- [23] A. Paulino and H. Araujo. Multiple robots in geometric formation: Control structure and sensing. In *International Symposium on Intelligent Robotic Systems*, pages 103–112, University of Reading, UK, July 2000.
- [24] E. Malis S. Benhimane. Vision-based control with respect to planar and non-planar objects using a zooming camera. In *IEEE International Conference on Advanced Robotics*, pages 863–869, July 2003.
- [25] C. Samson, B. Espiau, and M. Le Borgne. *Robot Control : The Task Function Approach*. Oxford University Press, 1991.
- [26] B. Thuilot, C. Cariou, P. Martinet, and M. Berducat. Automatic guidance of a farm tractor relying on a single cp-dgps. *Autonomous Robots*, 13, 2002.
- [27] Tomas Pajdla Tomas Svoboda and Vaclav Hlavac. Motion estimation using central panoramic cameras. In *IEEE Conference on Intelligent Vehicles*, Stuttgart, Germany, October 1998.
- [28] R. Vidal, O. Shakernia, and S. Sastry. Formation control of non-holonomic mobile robots with omnidirectional visual servoing and motion segmentation. In *IEEE International Conference on Robotics and Automation*, pages 584–589, Taipei, Taiwan, September 2003.
- [29] N. Winter, J. Gaspar, G. Lacey, and J. Santos-Victor. Omnidirectional vision for robot navigation. In *Proc. IEEE Workshop on Omnidirectional Vision, OMNIVIS*, pages 21–28, South Carolina, USA, June 2000.
- [30] Z. Zhang and A. R. Hanson. Scaled euclidean 3d reconstruction based on externally uncalibrated cameras. In *IEEE Symposium on Computer Vision*, Coral Gables, FL, 1995.